A Universal Relationship for Diffusion in Ternary Polymer Solutions: The Incompatible Polymers Polystyrene and Polyisobutylene in Benzene

Wyn Brown* and Pu Zhou

Institute of Physical Chemistry, University of Uppsala, Box 532, 751 21 Uppsala, Sweden

Received July 27, 1990; Revised Manuscript Received October 27, 1990

ABSTRACT: This paper reports self-diffusion coefficients determined by dynamic light scattering for polystyrene (PS, probe) in a polyisobutylene (PIB, matrix) over wide ranges of relative molecular weights of the two polymers with benzene as the solvent (Θ solvent for PIB at 24.5 °C). The refractive index of benzene is matched with that of PIB, resulting in single-exponential autocorrelation functions in the dynamic light scattering experiments. When the matrix chains are entangled, universal plots are found of the form $\log (DM)_{probe}$ versus $(C/C_e)_{matrix}$ over wide ranges of concentration of the matrix where C_e is the entanglement concentration. This relationship also applies both for $M_{probe} \gg M_{matrix}$ and $M_{probe} \ll M_{matrix}$. The previously used logarithmic diagrams of $(DM)_{probe}$ versus $(C/C^*)_{matrix}$ are also valid as universal plots but are less sensitive representations. At higher temperatures where there is increased mutual interpenetration of the PIB chains, the PS component is increasingly segregated from the matrix at progressively lower PIB concentrations. The effect is not simply related to C^*_{PIB}.

Introduction

There has been considerable interest in recent years in the dynamics of polymers in ternary systems: polymer$_1$ + polymer$_2$ + solvent. Although the techniques pulsed field gradient NMR[1,2] and forced Rayleigh scattering (FRS)[3,4] have been used to examine self-diffusion in the case where the two polymers differ only in molecular weight, dynamic light scattering (DLS) has been the favored technique in conjunction with "optical labeling".[5,6] Here one polymer (matrix polymer) of high relative concentration is chosen to be isorefractive with the solvent, while the other (probe polymer) is present at low concentration so that the measured diffusion coefficient derived from the single-exponential autocorrelation function is close to the self-diffusion coefficient of the probe. In particular, fairly compatible polymer pairs have been selected so that wide ranges of relative molecular weight and concentration could be employed primarily in order to test scaling predictions for self-diffusion, the assumption being made that the dynamics in the ternary system approximate those in the binary system. Subsequently, Borsali and co-workers[7,8] used a high relative concentration of the "visible" polymer and reported the presence of two modes. This was anticipated from the theory of Akcasu et al.[9] with subsequent development by Benmouna et al.[10] which predicts a bimodal autocorrelation function since the signal from one species will be modulated by that of the other. The modes are (1) the fast mode, corresponding to the cooperative diffusion coefficient characterizing the total polymer concentration fluctuations and which is identical with the cooperative diffusion coefficient measured in the binary system, and (2) the interdiffusion coefficient, which is a slow relaxation mode describing the relative motion of the two types of chain.

Recently, however, Akcasu[11] has shown that whereas two exponentially decaying modes represent the pure normal modes for the system, the cooperative and interdiffusion processes will correspond to mixed modes; i.e., the relaxation rates will be determined by the superposition of the pure modes.

In another approach, without recourse to refractive index matching. Brown and Zhou[12] employed DLS measurements on ternary systems in which the two polymers were chemically identical, differing only in molecular weight. The probe chain was maintained at a trace concentration and the matrix polymer concentration varied extensively in the semidilute range. It was shown that two modes could be isolated from the autocorrelation function by Laplace inversion, yielding the cooperative diffusion coefficient of the matrix and the self-diffusion coefficient of the probe (rather than the interdiffusion coefficient observed by Borsali et al.[7,8] when working at high relative concentrations of the two polymers). This was established by comparison of diffusion coefficients measured in the binary systems using DLS and pulsed field gradient NMR to measure self-diffusion. In this way it was found possible to avoid the troublesome perturbation of the dynamics of the probe arising from the nonperfect compatibility of the two types of chain. It is important to note the generality of this procedure for measuring a well-defined self-diffusion coefficient.

It was subsequently established[13] for widely varying relative molecular weights and concentrations that self-diffusion of the probe chain in a semidilute matrix follows the Rouse model to describe the effect of hydrodynamic screening. The topological effect of the matrix is compensated for by normalizing its concentration with the overlap concentration, C^*.[13,14] Thus a "universal" curve was found which describes the relationship between the diffusion of the probe and semidilute matrix concentration: i.e., $\log (DM)_{probe}$ versus $\log (C/C^*)_{matrix}$, where C^* is the coil overlap concentration. The data stand in opposition to reptation as a viable mechanism for self-diffusion in semidilute solutions since the same function also well described the diffusion of hard spheres in the system.[13]

Using the technique described, we have recently[15] extended the investigations to an incompatible polymer pair, viz., polystyrene (PS)/polyisobutylene (PIB) in chloroform as solvent. It was found that the probe chains are effectively segregated in the matrix polymer and progressively adopt the dynamics of the matrix chains. Normalization of the matrix polymer concentration with the entanglement concentration led to superposition of the data.

In the present investigation we employ a more conventional optical labeling geometry (PS/PIB/benzene) where the PIB matrix is isorefractive with benzene. The PS

0024-9297/91/2224-1820$02.50/0

probe is maintained low at trace concentration. As anticipated, the autocorrelation function is single exponential and then yields the self-diffusion coefficient of the probe. Our objective was to more systematically than previously explore self-diffusion in ternary systems when the chains possess limited compatibility. In particular, the influence of the relative molecular weights is examined. Furthermore, since benzene is a Θ solvent for PIB at 24.5 °C,[17] it becomes possible to examine the effect of a change in the solvent quality on probe diffusion.

Intensity light scattering has earlier been used to investigate the thermodynamic properties of ternary polymer systems, including the presently used incompatible polymers polystyrene/polyisobutylene.[16-21] The investigation of Hyde and Tanner[17,18] was, as here, limited to a low concentration of the "visible" polymer.

Experimental Section

Polyisobutylene samples were narrow-distribution fractions from Polymer Standards Service, Mainz, FRG. Polydispersity indices, molecular weights, and intrinsic viscosities were summarized in ref 15. Polystyrenes were from Pressure Chemical Co. ($M = 9 \times 1.0^5$, $M_w/M_n = 1.06$; $M = 4 \times 10^5$, $M_w/M_n = 1.03$) and Toya Soda Ltd. ($M = 8.4 \times 10^6$, $M_w/M_n = 1.02$; $M = 5 \times 10^6$, $M_w/M_n = 1.04$; $M = 2.95 \times 10^6$, $M_w/M_n = 1.03$). Stock solutions of the probe chains (≈0.05%) were first prepared, and these were used as the solvent for making the semidilute solutions of the matrix polymer. All solutions were filtered through 0.45-μm Millipore Durapore filters.

Dynamic Light Scattering. Measurements were made as previously described.[22] The autocorrelator was a multi-τ model (ALV-3000) from ALV, Langen, FRG, allowing 23 simultaneous sampling times and thus a monitoring of widely spaced decays in the same experiment. Laplace inversion was performed by using a constrained regularization routine (REPES)[23] to obtain the distribution of decay times. This program directly minimizes the sum of squared differences between the experimental and calculated correlation functions ($g^2(t)$) using nonlinear programming and allows selection of the parameter P: "probability to reject", which determines the degree of smoothing. The analysis of data, encompassing 191 exponentially spaced grid points and a grid density of 10 per decade, can be rapidly performed on an IBM-AT desk-top computer.

Static Light Scattering. Intensity light scattering measurements were made with a photon-counting device supplied by Hamamatsu. The light source was a 3-mW He–Ne laser (633 nm). The optical constant for vertically polarized light is $K = 4\pi n_0^2(dn/dC)^2/N_A\lambda^4$, where n_0 is the benzene refractive index and dn/dc is the refractive index increment (=0.105 mL/g in benzene at 25 °C and 633 nm). The scattering function, KC/R_θ, was measured on the same solutions as used for dynamic light scattering. R_θ is the Rayleigh ratio obtained by calibration measurements with benzene: $R_{90} = 8.5 \times 10^{-6}$ at 25 °C.[29]

Results and Discussion

Considerable progress has been made in recent years on the dynamics in ternary polymer systems. Attention has been focused on dynamic light scattering measurements of the diffusion of a linear chain within a matrix of the second (chemically different) polymer which is present at semidilute concentration and which has been selected so that its refractive index matches that of the solvent. When the test chain is present at sufficiently low concentration, the measured quantity should approximate the self-diffusion coefficient. However, it should also be recognized that, depending on the concentration dependence, it will differ from the self-diffusion coefficient determined, for example, for a spin-labeled chain as determined with pulsed field gradient NMR and which probably corresponds most closely to a rigorously defined self-diffusion coefficient. More critically for the interpretation of the experiments, it has been assumed[5,6] that the diffusion of the test chain will approximate that for the polymer in the semidilute binary polymer/solvent system and thus that various models, e.g., reptation, can be tested. This will apply only to the extent that there is complete molecular-level miscibility.

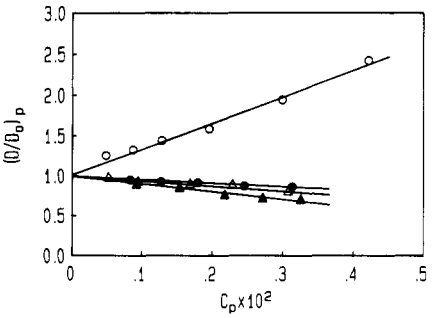

Figure 1. Dependence of the probe (PS(9×10^5)) diffusion coefficient in the matrix of PIB(3.8×10^6). Reduced probe diffusion coefficient D/D_0 against C_{probe}. The concentrations of matrix are 0% (○), 0.25% (●), 0.52% (△), and 0.98% (▲). C^*(PIB) = 0.34%.

Figure 1 shows the dependence of the reduced probe (PS) concentration, D/D_0, on the probe concentration for the binary polystyrene/benzene system and for several fixed concentrations of the PIB matrix extending up to about $3C^*$. C^* is defined here as $C^* = 3M/4\pi R_g^3 N_A$. A good experimental measure of C^* is the inverse intrinsic viscosity ($[\eta]^{-1}$) as shown in ref 31.

As noted for the chloroform system,[15] a very weak dependence of D_{probe} on its own concentration is observed, showing that the interactions between the PS chains are effectively screened by the PIB component. Since the concentration of the probe chain was 0.05% in all experiments, the measured quantity here approximates the self-diffusion coefficient of PS chains within the PIB matrix. This is an important point for the interpretation.

The two polymers used here are well-known to be incompatible and the anomalously low value of the polymer–polymer interaction parameter was discussed in the previous paper.[15] The radius of gyration of the PS coil was shown to remain approximately constant up to the vicinity of overlap of the PIB chains. It was concluded that the probe chains are effectively segregated in the matrix of the second polymer.

Figure 2A depicts the self-diffusion coefficients of PS(9×10^5) in PIB matrix compositions, varying in molecular weight from 1.1×10^6 to 4.9×10^6 in a logarithmic–linear plot against matrix concentration. Here, $M_{PS} < M_{PIB}$. It is noted that, in all cases in the present paper, relaxation rates are q^2 dependent. As concluded for the homopolymeric PIB_1/PIB_2 system,[12] the probe chain diffusion rate is strongly dependent on the matrix polymer molecular weight, but here there is a sharp upturn in D_{probe} which occurs at progressively lower matrix concentrations as the molecular weight increases. Figure 2B shows that the curves superimpose when the matrix concentration is normalized with its entanglement concentration, C_e. $C_e = \rho M_e/M$, where ρ is the polymer density, M_e is the molecular weight between entanglements (8600 for PIB),[24] and M is the molecular weight of the chain.

Through the Stokes–Einstein equation, it is reasonable to correlate the diffusion coefficient of the probe in a polymer solution of concentration C with the macroscopic viscosity of the solution and hence C^* since it is well-known from both theory[32,33] and experiment[34] that the macroscopic shear viscosity depends only on C/C^* and is independent of M. However, the motions of the probe chain are expected to be more directly coupled with the

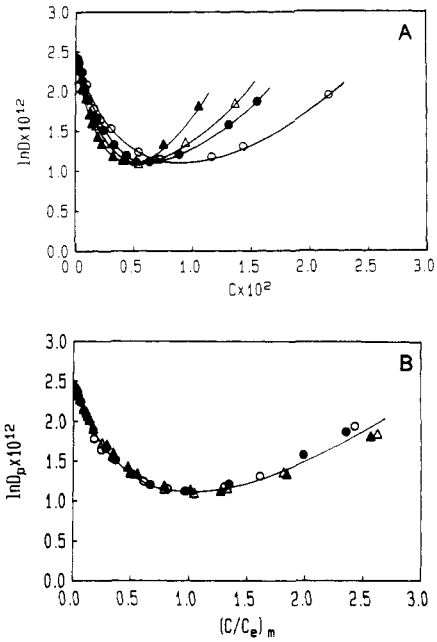

Figure 2. Self-diffusion coefficients for the polystyrene probe ($M = 9 \times 10^5$) in polyisobutylene solutions in benzene at 24.5 °C ($M_{PIB} = 1.1 \times 10^6$ (○), 1.9×10^6 (●), 3.8×10^6 (△), and 4.9×10^6 (▲). In (B) the PIB concentration is normalized with its entanglement concentration.

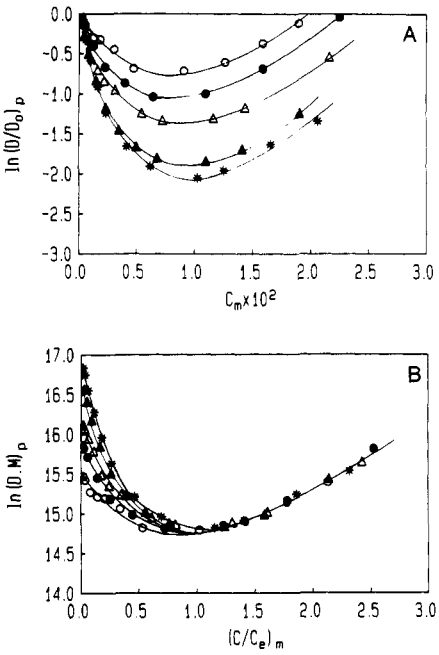

Figure 3. Self-diffusion of polystyrene probe chains of various molecular weights in polyisobutylene matrix solutions in benzene at 24.5 °C ($M_{PIB} = 1.1 \times 10^6$). $M_{PS} = 1.67 \times 10^5$ (○), 4×10^5 (●), 9×10^5 (△), 2.95×10^6 (▲), and 5×10^6 (*). The data (B) have the PIB concentration normalized with its entanglement concentration (C_e) and the probe self-diffusion coefficient multiplied by its molecular weight.

entanglement density determining the structure and properties of entangled solutions. Thus an alternative is to normalize the matrix concentration with the entanglement concentration. As shown in the previous paper,[15] this is illuminating for polymer mixtures of limited compatibility.

Figure 3A shows a similar plot to that in Figure 2 but for data obtained when the PS probe molecular size is varied between 1.67×10^5 and 5×10^6, holding the PIB matrix constant ($M = 1.1 \times 10^6$). These experiments cover the situation from where, on the one hand, the probe is

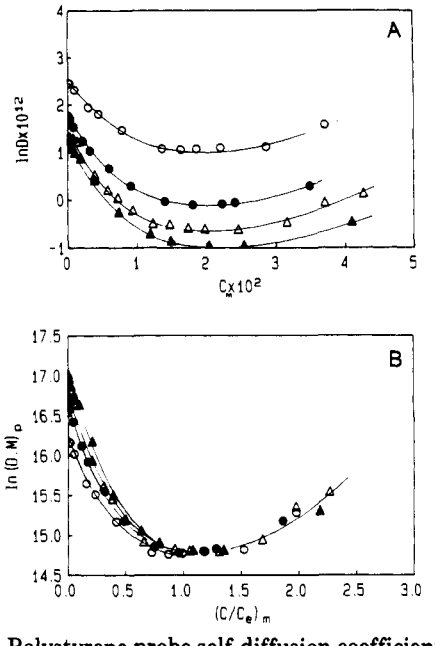

Figure 4. Polystyrene probe self-diffusion coefficients plotted versus concentration of the polyisobutylene matrix in benzene at 24.5 °C ($M_{PIB} = 2.47 \times 10^5$). $M_{PS} = 9 \times 10^5$ (○), 2.95×10^6 (●), 5×10^6 (△), and 7×10^6 (▲). In (B) is the analogous log (DM) versus (C/C_e) plot to that in Figure 2B.

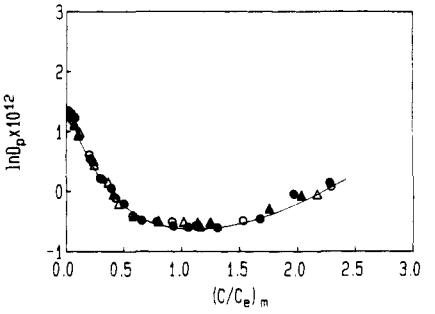

Figure 5. Self-diffusion coefficients for polystyrene ($M = 5 \times 10^6$) in polyisobutylene solutions in benzene at 24.5 °C plotted versus (C/C_e) for the PIB matrix. $M_{PIB} = 1.82 \times 10^5$ (○), 2.47×10^5 (●), 6.1×10^5 (△), and 8.56×10^5 (▲).

significantly smaller than the matrix to the other extreme where the probe is much larger than the matrix chains. Figure 3B shows the data with the matrix concentration normalized with C_e and the probe self-diffusion coefficient multiplied by its molecular weight. As shown before,[15] above the matrix entanglement concentration (overlap concentration) screening of the hydrodynamic interactions follows the Rouse model for freely draining coils with no entanglements. In the dilute, unentangled, range below C_e the curves diverge as would be anticipated. It may be noted that both Rouse and Zimm models are formulated in terms of the binary polymer/solvent system. In ternary systems with two polymer species as dealt with here, the molecular weight in the relationships $D \sim M^{-1}$ (Rouse) and $D \sim M^{-\nu}$ (Zimm) refers to that of the probe chain.

In the third data set displayed in Figure 4A, four different molecular weights of the PS probe are employed in conjunction with PIB matrix chains of low molecular weight ($M = 2.47 \times 10^5$). The corresponding log (DM) versus (C/C_e) plot is given in Figure 4B.

Figure 5 shows data with a constant PS probe molecular weight ($M = 5 \times 10^6$) in PIB matrices differing in M from 1.82×10^5 to 8.56×10^5, i.e., $M_{PS} > M_{PIB}$ in all cases (compare Figure 2).

Figure 6 collects the data for two PS probes in a variety of molecular weights of the PIB matrix.

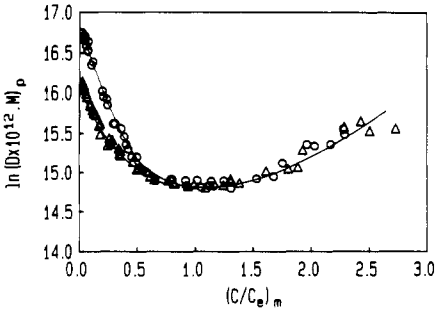

Figure 6. Data for polystyrene probes ($M = 9 \times 10^5$ (△) and 5×10^6 (○)) in polyisobutylene solutions in benzene at 24.5 °C. The data are those shown in Figures 2B and 5 and are plotted here in the format log $(DM)_{probe}$ versus $(C/C_e)_{matrix}$.

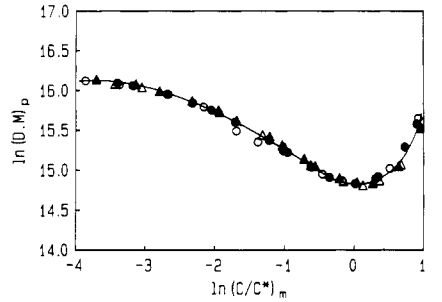

Figure 7. log (DM) versus (C/C^*) plots for the data in Figure 2B.

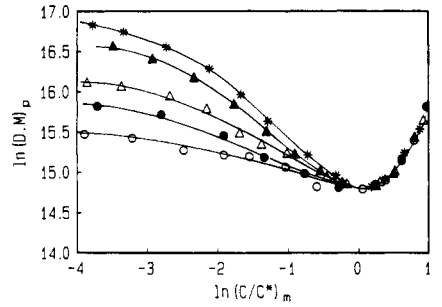

Figure 8. log (DM) versus (C/C^*) plots for the data in Figure 3.

Taken together, the above data for a wide range of relative molecular weights of probe and matrix establish that log (DM) versus (C/C_e) plots form a universal curve over wide ranges of concentration of the matrix chains in the entangled region. It is not yet clear, however, whether C_e is to be preferred over C^* for normalizing the matrix concentration since, for the present samples, the entanglement concentration is similar in magnitude to the overlap concentration.

The earlier papers[12] dealing with the homopolymeric PIB_1/PIB_2 system showed a good correlation between log $(DM)_{probe}$ and log $(C/C^*)_{matrix}$. Taking the data from Figure 2 for various sizes of the matrix chain together with a fixed probe size, it is shown in Figure 7 that a similar excellent correlation exists using plots of this type with incompatible polymers. Furthermore, it is shown in Figure 8 that almost precise superposition is achieved when the overlap concentration is exceeded for the data given in Figure 3 where, instead, the probe chain is varied in size. The generality of the log (DM) versus (C/C^*) plots can be established by comparison with data for self-diffusion using another technique. Figure 9A shows data for the homopolymeric PS_1/PS_2/chloroform systems where the matrix molecular weight is maintained constant (2.95×10^6) and the probe chains are varied from 1.15×10^5 up to 7×10^6. The universal plot (for a given polymer/solvent

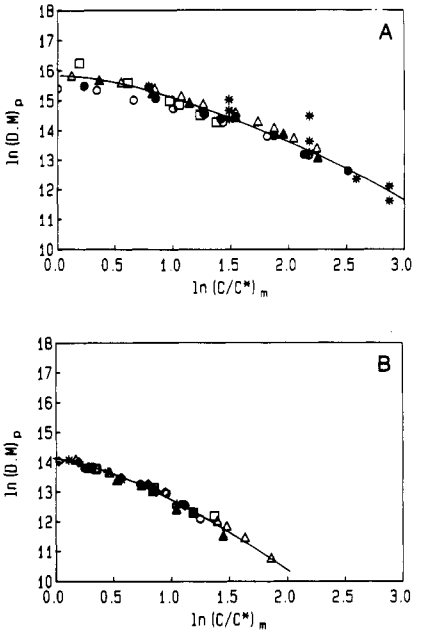

Figure 9. (A) log (DM) versus (C/C^*) plots for homopolymeric polystyrene systems in chloroform at 25 °C. Matrix: PS $M = 2.95 \times 10^6$; probes: PS $M = 1.15 \times 10^5$ (○), 1.67×10^5 (●), 5.98×10^5 (△), 9×10^5 (▲), and 7×10^6 (□). The data represented with asterisks are from Kim et al.[3] and are for polystyrenes in toluene. (B) Data for the homopolymeric polyisobutylene systems shown in a plot as in (A) [$1.82 \times 10^5/4.9 \times 10^6$ (○), $2.47 \times 10^5/4.9 \times 10^6$ (●), $6.1 \times 10^5/4.9 \times 10^6$ (△), $8.56 \times 10^5/4.9 \times 10^6$ (▲), $4.9 \times 10^6/8.04 \times 10^4$ (◆); $4.9 \times 10^6/1.82 \times 10^5$ (◇), $4.9 \times 10^6/2.47 \times 10^5$ (*), $4.9 \times 10^6/6.1 \times 10^5$ (□), $4.9 \times 10^6/1.1 \times 10^6$ (■), where the various combinations are probe/matrix molecular weights].

system) is also shown to be applicable here. Included on the diagram are self-diffusion data for polystyrenes in toluene obtained by Kim et al.[3] using forced Rayleigh scattering. The agreement is gratifying. Such plots should not be expected to superimpose for polymers which are structurally different, since, for example, the dependence of the screening of the hydrodynamic interactions on molecular weight will differ for chains having different backbone structure. This is illustrated by comparing Figure 9A for PS systems with Figure 9B for the homopolymeric PIB system. M_{probe} will presumably be replaced by $f(N,\zeta)$, where N is the number of probe chain units and ζ the friction coefficient per monomer.

Figure 10A shows the effect of change in solvent quality in the PS/PIB/benzene system with a shift in temperature from 24.5 °C (Θ system for PIB/benzene) to 55 °C. At higher temperature, there will be greater interpenetration of the PIB coils, and thus the PS chains will be segregated from the PIB at increasingly lower concentrations of PIB as is clear in this figure. Attempting to reduce these data as before using normalization of the PIB concentration with C^* is only partially successful, however (Figure 10B).

We conclude, as before, that the topological effect of the matrix may be described by employing the reduced concentration (C/C^*) or alternatively (C/C_e). For a given polymer(s), the hydrodynamic screening effect for overlapped and entangled coils is given by M_p^{-1}.

The above data clearly show that the minima in the curves (e.g., those in Figures 2 and 3) coincide with the onset of entanglement in the matrix polymer. Since probe and matrix chains cannot entangle due to incompatibility, segregation of the PS probe results. Qualitatively, it seems reasonable to assume that the local confinement of the probe within the matrix will mean its entrapment and

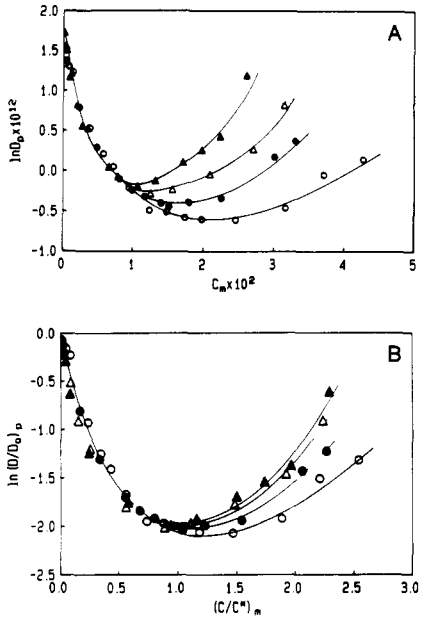

Figure 10. (A) Temperature dependence of probe diffusion (probe, PS(4.9×10^6); matrix, PIB(2.47×10^5)) at the following temperatures: 24.5 °C (○) (Θ conditions for PIB); 35 °C (●); 45 °C (△); 55 °C (▲). In (B) are shown the data in (A) as log $(D/D_0)_{probe}$ versus log $(C/C^*)_{matrix}$.

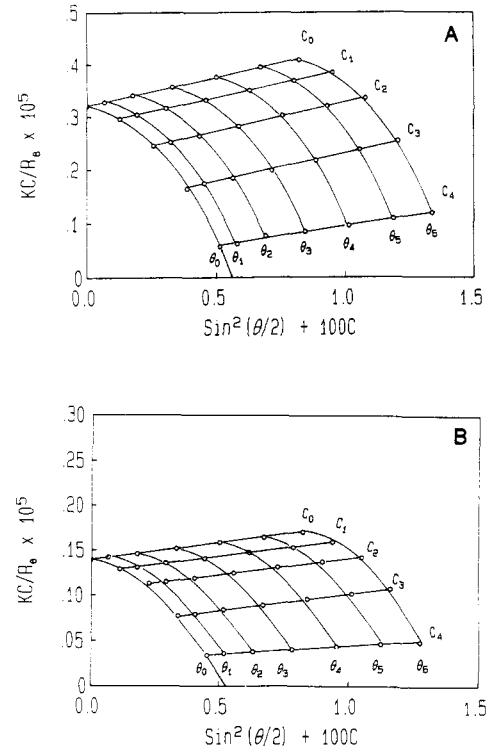

Figure 11. (A) Zimm-type diagrams for PS($M = 9 \times 10^5$) and PIB($M = 3.8 \times 10^6$) in benzene. C_{PIB}: C_0, 0; C_1, 1.3×10^{-3}; C_2, 2.6×10^{-3}; C_3, 3.85×10^{-3}; C_4, 5.14×10^{-3} g/mL. $C_{PS} = 6.4 \times 10^{-4}$ g/mL. Angles: 0 = 0°; 1 = 30°; 2 = 50°; 3 = 70°; 4 = 90°; 5 = 110°; 6 = 130°. (B) Zimm-type diagrams with PS($M = 8 \times 10^6$) and PIB($M = 3.8 \times 10^6$) in benzene. C_{PIB}: C_0, 0; C_1, 1.1×10^{-3}; C_2, 2.3×10^{-3}; C_3, 3.4×10^{-3}; C_4, 4.5×10^{-3} g/mL. $C_{PS} = 6.4 \times 10^{-4}$ g/mL. Angles: As in Figure 11A.

that it will progressively adopt the faster cooperative motions of the matrix segments as the concentration of the latter is increased. Thus the probe motions will increasingly reflect those of the matrix (although the latter is "invisible" due to refractive index matching).

As shown in the previous paper[15] using intensity light scattering, the pronounced increase in D_{probe} above C_e is not attributable to a contraction in the probe coil size. Rather, the apparent radius of gyration, $(R_g)_{app}$, observed at low C_{PIB} and determined at low q values is approximately constant (see below).

We have employed static light scattering to further elucidate the interactions in the system. These data are shown in Figure 11 in the form of Zimm plots for PS fractions having molecular weights, respectively, much smaller than and greater than that of the PIB matrix. It should be noted that these diagrams only use the formalism of a conventional Zimm plot for a binary system and that the data have been plotted in this way for convenience in representation. In a ternary system, the expressions for the reduced intensity are complicated.[18] The intercept on the vertical axis gives an apparent molecular weight for the PS at the concentration used, while the $(KC/R_\theta)_{\theta=0}$ line versus the total polymer concentration reflects the interactions in the system and becomes progressively more negative as the spinodal is approached with increasing PIB concentration. The angular dependence at each PIB concentration, divided by the reciprocal molecular weight of the PS, is assumed to a first approximation to yield R_g^2 for PS since in benzene PIB gives a negligible contribution to the scattered intensity. These plots have an unusual and characteristic shape. Ould Kaddour and Strazielle[26] applied a mean field theory of Benoit and Benmouna[27,28] and showed for the similar system PS/PDMS/THF in which the latter two components are refractive index matched that it accounts quantitatively for the distortion of the angular dependence of scattered light. The spinodal composition (at which the light scattering from the homogeneous phase goes to infinity) is found from the intercept of the Θ = 0 line with the horizontal axis. The present systems differ from those in the earlier investigations in that the polystyrene concentration is maintained very low (≈0.06%). The polymer–polymer interaction parameter ($\chi_{2,3}$) (Table I) maintains a low value, in keeping with the results of the earlier investigations and, although in these two systems one might anticipate differing extents of coil interpenetration, this parameter is rather insensitive to the relative molecular weights of probe and matrix.

Table I
Spinodal Compositions and PS/PIB Interaction Parameters

system	$\phi_3 \times 10^2$	$\phi_2 \times 10^2$	$\chi_{2,3}$[a]
PS(9×10^5)/PIB(3.8×10^6)	0.74	0.06	0.0231
PS(8.4×10^6)/PIB(3.8×10^6)	0.54	0.06	0.0297

[a] $\chi_{2,3} - \chi_{1,2} - \chi_{1,3} = -1/\phi_1 + [(1/\phi_1 + 1/m_2\phi_2 - 2\chi_{1,2})(1/\phi_1 + 1/m_3\phi_3 - 2\chi_{1,3})]^{0.5}$), taken from ref 30. The $\chi_{i,j}$ are interaction parameters; m_i is the weight fraction and ϕ_i the volume fraction of component i at the spinodal. Component 1 = solvent; 2 = polystyrene; 3 = polyisobutylene.

The slope of the line $C = 0$ gives an apparent radius of gyration $(R_g)_{app}$ for the PS chain at $C_{PIB} = 0$. It is clear that as C_{PIB} changes, there is only a small change in $(R_g)_{app}$, as concluded by Hyde and Tanner.[17,18] This finding supports the previous conclusion[15] that the two types of chain segregate in solution. The interactions between the PS chains are effectively screened by the PIB. At higher concentrations, $(R_g)_{app}$ shows an increase,[15] the apparent radius being strongly influenced by the properties of the mixture. Kappeler et al.[35] have recently applied renormalization group theory to ternary polymer systems and make an analysis of $(R_g)_{app}$. A parameter-free prediction of $(R_g)_{app}$ is made that almost precisely fits the experimental data.

Although there is as yet no theoretical model for predicting the influence of polymer incompatibility on

transport properties in such systems, it is hoped that the present data will assist in providing an experimental framework for such development.

Acknowledgment. Financial support from the Swedish Natural Science Research Council (NFR) and the Swedish National Board for Technical Development (STU) is gratefully acknowledged.

References and Notes

(1) Callaghan, P. T.; Pinder, D. N. *Macromolecules* **1984**, *17*, 431.
(2) von Meerwall, E. D.; Amis, E. J.; Ferry, J. D. *Macromolecules* **1985**, *18*, 260.
(3) Kim, H.; Chang, T.; Yohanan, J. M.; Wang, L.; Yu, H. *Macromolecules* **1986**, *19*, 2744.
(4) Wesson, J. A.; Noh, I.; Kitano, T.; Yu, H. *Macromolecules* **1984**, *17*, 782.
(5) Lodge, T. P. *Macromolecules* **1983**, *16*, 1393; **1986**, *19*, 2986.
(6) Martin, J. E. *Macromolecules* **1984**, *17*, 1279; **1986**, *19*, 922, 1278.
(7) Borsali, R.; Duval, M.; Benmouna, M. *Polymer* **1989**, *30*, 610.
(8) Borsali, R.; Duval, M.; Benmouna, M. *Macromolecules* **1989**, *22*, 816.
(9) Akcasu, A. Z.; Hammouda, B.; Lodge, T. P.; Han, C. C. *Macromolecules* **1984**, *17*, 759.
(10) Borsali, R.; Duval, M.; Benoit, H.; Benmouna, M.; Akcasu, A. Z. *Macromolecules* **1987**, *20*, 1107, 1112.
(11) Akcasu, A. Z., personal communication.
(12) Brown, W.; Zhou, P. *Macromolecules* **1989**, *22*, 890, 3508, 4031.
(13) Brown, W.; Zhou, P. *Polymer* **1990**, *31*, 772.
(14) Nemoto, N.; Okada, S.; Inoue, T.; Kurata, M. *Macromolecules* **1988**, *21*, 1502, 1509.
(15) Brown, W.; Zhou, P. *Macromolecules* **1990**, *23*, 5097.
(16) Allen, G.; Gee, G.; Nicholson, J. P. *Polymer* **1960**, *1*, 56.
(17) Hyde, A. J.; Tanner, A. G. *J. Colloid Interface Sci.* **1968**, *28*, 170.
(18) Hyde, A. J. In *Light Scattering from Polymer Solutions*; Huglin, M. B., Ed.; Academic Press: London, 1972; Chapter 10.
(19) Van den Esker, M. W. J.; Vrij, J. *J. Polym. Sci., Polym. Phys. Ed.* **1976**, *14*, 1943, 1953, 1967.
(20) Kuhn, R.; Cantow, H.-J.; Burchard, W. *Angew. Makromol. Chem.* **1968**, *2*, 14.
(21) Nagata, M.; Fukuda, T.; Inagaki, H. *Macromolecules* **1987**, *20*, 2173.
(22) Nicolai, T.; Brown, W.; Johnsen, R. M.; Stepanek, P. *Macromolecules* **1990**, *23*, 1165.
(23) Jakes, J., to be published.
(24) Ferry, J. D. *Viscoelastic Properties of Polymers*; Wiley: New York, 1980.
(25) Phillies, G. D. J. *J. Chem. Phys.* **1983**, *79*, 2325.
(26) Ould Kaddour, L.; Strazielle, C. *Polymer* **1987**, *28*, 459.
(27) Benoit, H.; Benmouna, M. *Polymer* **1984**, *25*, 1059.
(28) Benoit, H.; Benmouna, M. *Macromolecules* **1984**, *17*, 535.
(29) Pike, E. R.; Pomeroy, W. R. M.; Vaughan, J. M. *J. Chem. Phys.* **1975**, *62*, 3188.
(30) Koningsveld, R.; Chermin, H. A. G.; Gordon, M. *Proc. R. Soc. London* **1970**, *A319*, 331.
(31) Brown, W.; Mortensen, K. *Macromolecules* **1988**, *21*, 420.
(32) de Gennes, P.-G. *Scaling Concepts in Polymer Physics*; Cornell University Press: Ithaca, NY, 1979.
(33) Doi, M.; Edwards, S. F. *The Theory of Polymer Dynamics*; Clarendon: Oxford, 1986.
(34) Adam, M.; Delsanti, M. *J. Phys. (Les Ulis, Fr.)* **1983**, *44*, 1185.
(35) Kappeler, C.; Schäfer, L.; Fukuda, T. Personal communication.

Registry No. PS, 9003-53-6; PIB, 9003-27-4; benzene, 71-43-2.